analytical chemistry

ARTICLE

pubs.acs.org/ac

Graphene Oxide Based Photoinduced Charge Transfer Label-Free Near-Infrared Fluorescent Biosensor for Dopamine

Jin-Long Chen,[†] Xiu-Ping Yan,*[,†] Kang Meng,[‡] and Shu-Feng Wang[‡]

[†]State Key Laboratory of Medicinal Chemical Biology, and Research Center for Analytical Sciences, College of Chemistry, Nankai University, Tianjin 300071, China

[‡]State Key Laboratory for Mesoscopic Physics, School of Physics, Peking University, Beijing 100871, China

Supporting Information

ABSTRACT: While the super fluorescence quenching capacity of graphene and graphene oxide (GO) has been extensively employed to develop fluorescent sensors, their own unique fluorescence and its potential for chemo-/biosensing have seldom been explored. Here we report a GO-based photoinduced charge transfer (PCT) label-free near-infrared (near-IR) fluorescent biosensor for dopamine (DA). The multiple noncovalent interactions between GO and DA and the ultrafast decay at the picosecond range of the near-IR fluorescence of GO resulted in effective self-assembly of DA molecules on the surface of GO, and significant fluorescence quenching, allowing development of a PCT-based biosensor with direct readout of the near-IR fluorescence of GO for selective and sensitive detection of DA. The developed method gave a detection limit of 94 nM and a relative standard deviation of 2.0% for 11 replicate detections of 2.0 μM DA and was successfully applied to the determination of DA in biological fluids with quantitative recovery (98−115%).

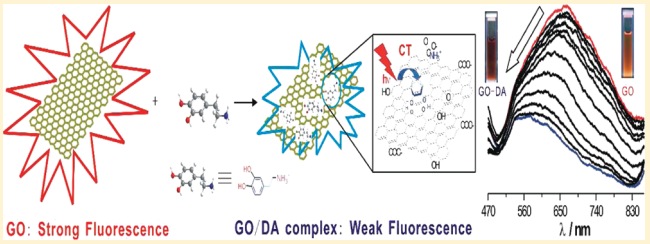

Graphene oxide (GO) holds great potential for optical biosensors because of its remarkable characteristics such as sp^2/sp^3 coexisting structure,[1−3] high mechanic strength,[4] good water dispersibility,[5,6] facile surface modification,[7−9] and super fluorescence quenching capacity.[10,11] Since the first application of GO as fluorescence resonance energy transfer (FRET) biosensor,[12] great attention has been paid to the development of GO-based sensors for DNA,[13−16] protein,[17] ATP,[18] duplex-DNA unwinding,[19] glucose,[20,21] and metal ions.[22] The observed electrogenerated chemiluminescence[23] and photoluminescence originating from the pristine graphene[24−26] and chemically prepared GO[27−30] offer new exciting opportunities in bionanotechnology such as cell imaging and chemo-/biosensing. Most of GO-based fluorescent sensors have been elaborately designed on the basis of FRET from a specific fluorescent dye-labeled probe to GO by employing the super quenching capacity of GO.[12−20,22] To date, few GO-based biosensors on the direct readout of the fluorescence of GO based on FRET from GO to a specific quencher (Au nanoparticles) have been reported.[31,32] However, the above-mentioned GO-based optosensors by utilizing either the super quenching capacity or the fluorescence property of GO usually render several limitations such as complex, high-cost, and time-consuming fluorescence labeling and multiple steps of chemical modification. To the best of our knowledge, no GO-based photoinduced charge transfer (PCT) optosensors with direct readout of the fluorescence of GO have been reported so far.

We are interested in direct utilization of the near-infrared (near-IR) fluorescence of GO to develop label-free biosensors for detecting biomarkers based on the PCT mechanism. Interest in near-IR fluorescent biosensors is increasing because such biosensors operating in the near-IR region can avoid interference from biological media such as tissue autofluorescence and scattering light, thereby facilitating relatively interference-free sensing.[33]

Here we show the first example of GO-based label-free PCT biosensors for biomolecules. To demonstrate the proof-of-concept, we chose dopamine (DA) as the target because it is an important catecholamine neurotransmitter.[34,35] The level of DA and its related compounds in biological fluids reflects the biodegradation efficiency of aromatic amino acids, especially tyrosine, playing an important role in clinical diagnosis.[36] However, detection of DA in biological matrixes usually suffers interference from other aromatic acids, amino acids, other catecholamine neurotransmitters, particularly ascorbic acid (AA), and uric acid (UA).[37,38] Therefore, it is challenging to detect DA in biological matrixes selectively without the aid of a separation procedure. In this work, a novel label-free GO-based label-free PCT biosensor was developed for sensitive and selective detection of DA in biological fluids.

EXPERIMENTAL SECTION

Chemicals and Materials. All of the chemicals used are at least of analytical grade. Natural graphite flakes were obtained from Qingdao Henlide Graphite Co. (Qingdao, China) with an

Received: September 5, 2011
Accepted: October 6, 2011
Published: October 06, 2011

dx.doi.org/10.1021/ac2023537 | *Anal. Chem.* 2011, 83, 8787–8793

average particle size of 20 μm. $KMnO_4$, HCl, H_2SO_4, $NaNO_3$, and tris(hydroxymethyl)aminomethane (Tris) were obtained from Tianjin Kaitong Chemicals Co. (Tianjin, China). Ascorbic acid, urea acid, and catechol were purchased from the First Chemicals Co. of Tianjin (Tianjin, China). Dopamine hydrochloride and L-DOPA were purchased from Tianjin Guangfu Chemicals Co. (Tianjin, China). A Tris-HCl buffer solution (5.0 mM, pH 5.0) was used in the experiments. Ultrapure water (18.2 MΩ cm) obtained from a Water Pro water purification system (Labconco Corp., Kansas City, MO, USA) was used throughout this work.

Preparation of Vis−Near-IR Fluorescent Graphene Oxide Nanosheets. GO was synthesized from natural graphite flakes according to a modified Hummers method.[39,40] In a typical preparation, to a glass beaker 0.5 g of graphite flakes, 0.5 g of $NaNO_3$, and 23 mL of 98% (w/w) H_2SO_4 were added and mixed under stirring in an ice bath. Then, 3 g of $KMnO_4$ was slowly added to the mixture in an ice bath and thoroughly mixed. The beaker was placed in a water bath at 35 °C, and the solution was stirred for about 1 h to form a thick paste. A 40 mL aliquot of ultrapure water was added to the formed paste and stirred at 90 °C for 35 min. Finally, 100 mL of ultrapure water was added, followed by a slow addition of 3 mL of 30% (w/w) H_2O_2; meanwhile the color of the solution turned from dark brown to yellow. The warm solution was then filtered and washed with 100 mL of ultrapure water. The obtained cake was then dispersed in ultrapure water by mild sonication for 1 h. The suspension was centrifuged at 1000 rpm for 5 min. The supernatant was collected for centrifugation at 1000 rpm for 5 min (3−5 times) to remove all visible particles. The supernatant was collected and then centrifuged at 10 000 rpm for 15 min twice. The supernatant containing small GO pieces and water-soluble byproducts was discarded, while the sediment was collected. The solid GO was obtained from the sediment under air-dry. The slurry or solution of GO was obtained by re-dispersing the as-made GO in ultrapure water under mild sonication using a table-top ultrasonic cleaner. The freshly prepared GO suspension showed a considerable fluorescence emission at 600 nm.

To obtain the near-IR fluorescence of GO at 660 nm, a mixture (30 mL) of freshly prepared GO suspension and concentrated H_2SO_4 by a ratio of 3:5 (v/v) was heated at 60 °C for 4 h. The mixture was then diluted with ultrapure water (250 mL) and then centrifuged at 10 000 rpm for 5 min. The sediment was collected and re-dispersed into ultrapure water. The homogeneous colloidal solution of GO was centrifuged at 12 000 rpm for 15 min. The above-described procedures were repeated for five times to remove residual acid. All of the prepared GO samples showed good dispersity and stability in water.

Instrumentation and Characterization. The UV−vis absorption spectra were recorded on a Shimazu UV-3600 UV−vis−near-IR spectrophotometer at room temperature. The structure and morphology of GO and the GO−DA complex were characterized on a JEOL-100CXII transmission electron microscope with an accelerating voltage of 100 kV. Tapping mode atomic force microscopy (AFM) measurements were performed on a Multimode SPM with a Nanoscope IIIa controller from Digital Instruments. The samples for AFM images were prepared by depositing a diluted water dispersion of GO and the GO−DA complex on a freshly cleaved mica surface and allowing it to dry under ambient conditions.

All fluorescence measurements were performed on a Hitachi F-4500 fluorescence spectrophotometer equipped with a plotter unit and a 1 cm quartz cell. All fluorescence titration experiments were carried out in a 25 μg mL^{-1} GO water solution as a probe in pH 5 Tris-HCl buffer solution (5 mM) at room temperature if not otherwise indicated. All data were collected under the following conditions: PMT voltage, 950 V; excitation and emission slits, 10 nm; response, 2 s.

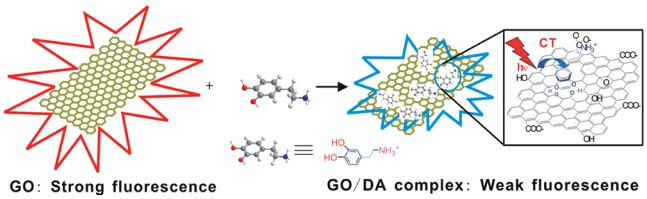

Figure 1. Schematic illustration for the developed GO-based photoinduced charge transfer fluorescent biosensor for DA.

The time-resolved fluorescence spectra were collected with a Hamamatsu C5680 synchroscan streak camera. The sample solutions were placed in 1 mm thick rotating cells to avoid photobleaching. The samples were excited by a frequency doubled Ti:sapphire laser pulse (Mira 900F, Coherent, Santa Clara, CA, USA) at 415 nm. The pulse width was about 120 fs, and the repetition rate was 76 MHz. The fluorescence was collected at magic angle (54.7°) polarization with respect to the excitation beam to avoid the anisotropic effects. The temporal scanning range was selected as 160 ps with an instrument response function (IRF) of 4 ps.

Sample Collection and Pretreatment. Two human serum samples and two human urine samples were collected from healthy adult volunteers. All samples were subjected to a 100-fold dilution before analysis, and no other pretreatments were necessary.

Measurement Procedures. To a 10 mL calibrated test tube, Tris-HCl buffer (50 mM, 1 mL, pH 5.0), GO solution (0.5 mg mL^{-1}, 0.5 mL), and certain amounts of DA standard solution or sample (0.5 mL) were sequentially added. The mixture was diluted to volume with ultrapure water, mixed thoroughly, and incubated in a water bath (35−40 °C) for 10 min. Then, the mixture was taken out from the water bath and allowed to cool to room temperature for 5 min for fluorescence measurements at an excitation wavelength of 450 nm and an emission wavelength of 660 nm.

RESULTS AND DISCUSSION

Label-Free GO-Based Optosensing Strategy. The principle for the present GO-based label-free PCT biosensors for DA is illustrated in Figure 1. A graphene-network functionalized with oxygen-containing groups including hydroxyl, carboxyl, and epoxide groups not only makes GO have good water solubility and stability but also enables noncovalent interaction with diols, amine functional groups, and phenyl in DA through electrostatic interaction, $\pi-\pi$ stacking, and hydrogen bonding to multiply recognize DA with high specificity. Such direct interaction of GO with DA effectively quenched the near-IR fluorescence of GO based on a PCT mechanism, allowing specific detection of DA in biological samples.

Fluorescence Quenching of GO Colloids by DA. A red-brown of GO water colloid displayed optical properties typical of chemically prepared GO, with two characteristic absorption peaks at 230 and 300 nm originating from $\pi-\pi^*$ transition of

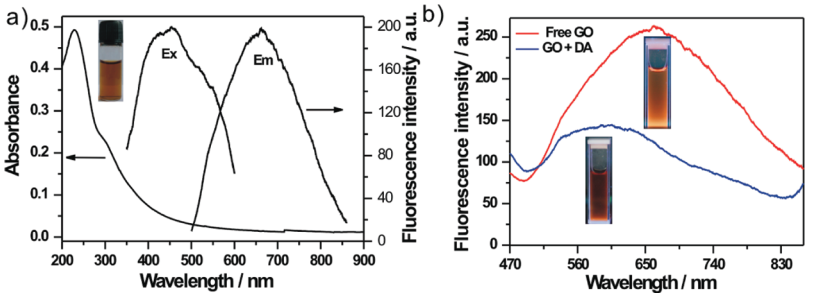

Figure 2. (a) UV−vis−near-IR absorption and fluorescence spectra of GO aqueous solution (inset: photograph for GO solution under sunlight); (b) changes of 25 μg mL^{-1} GO fluorescence excited at 450 nm in the presence (lower) and absence (upper) of 25 μM DA with a visible fluorescence color change in a pH 5.0 of 5.0 mM Tris-HCl solution under irradiation of 365 nm light.

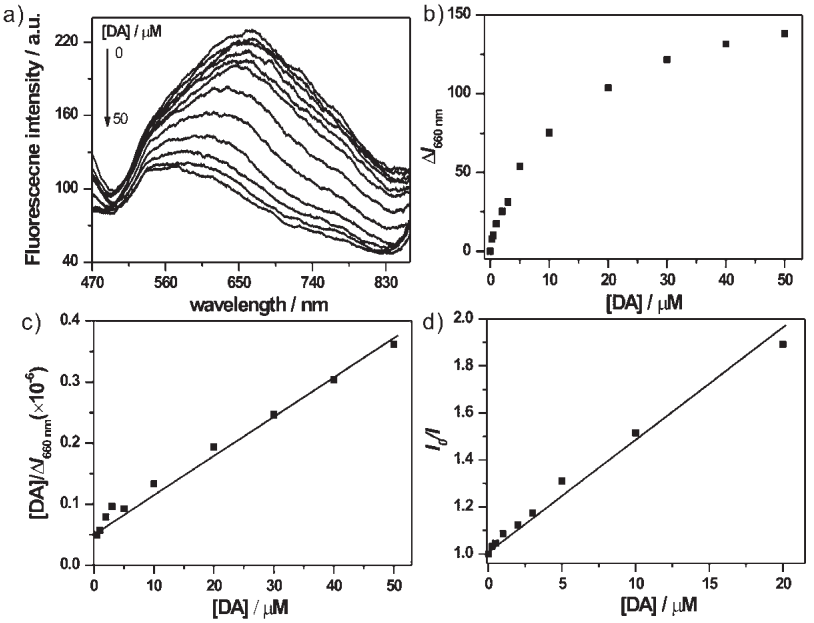

Figure 3. (a) Fluorescence spectra of 25 μg mL^{-1} GO solution under excitation at 450 nm in the presence of various DA concentrations in a pH 5.0 of 5.0 mM Tris-HCl solution (0, 0.25, 0.5, 1.0, 2.0, 3.0, 5.0, 10, 20, 30, 40, and 50 μM); (b) plot of the quenched fluorescence intensity at 660 nm (ΔI) versus DA concentration ([DA]); (c) plot of [DA]/ΔI against [DA], showing a linear fit to the Langmuir adsorption isotherm; (d) plot of I_0/I against [DA], showing a linear fit to the Stern−Volmer equation.

the C=C band and n−π^* transition of the C=O band, respectively (Figure. 2a),[41] and a strong fluorescence emission centered at 660 nm profiling from visible to near-infrared field under excitation of 450 nm light with a quantum yield of 0.5% presumably resulting from the radiative recombination of electron−hole pairs localized within sp^2 domains embedded in the sp^3 matrix.[27,29]

Addition of DA to the aqueous solution of GO led to a significant quenching of the near-IR fluorescence of GO with an obvious blue shift of the maximum emission wavelength from 660 to 590 nm within 5 min (Figure. 2b). Moreover, DA gave a steady and maximal quenching effect on the near-IR fluorescence of GO in a wide pH range from 4.5 to 7.0 (Figure S1 in the Supporting Information) because of high affinity between anionic GO and positively charged DA molecules (pI 9.7).[42] A significant reduction of the ζ potential from −36 eV of free GO to −25 eV of GO in the presence of 30 μM DA at pH 5.0 showed a predominant electrostatic interaction between GO and DA. Considering the strong fluorescence of free GO under acidic conditions,[43] a pH 5.0 Tris-HCl buffer solution (5.0 mM) was recommended throughout our experiments.

The change of the fluorescence intensity (ΔI) of GO at 660 nm was of DA concentration ([DA]) dependence (Figure 3). ΔI increased linearly with the concentration of DA at low concentrations of DA and then gradually leveled off at higher concentrations of DA. The adsorption of DA molecules onto the GO surface followed the Langmuir adsorption isotherm (Figure 3c):

$$\frac{[\mathrm{DA}]}{\Delta I} = \frac{[\mathrm{DA}]}{\Delta I_{\max}} + \frac{K_\mathrm{d}}{\Delta I_{\max}} \quad (1)$$

where K_d is the dissociation constant of the GO−DA complex and $\Delta I_{\max}$ is the fluorescence change at saturation. The K_d was estimated to be 1.2 × 10^{-5} M from the Langmuir adsorption isotherm in Figure 3c. The above results indicate that DA molecules were adsorbed onto the GO surface as a monolayer or sub-monolayer,[45] agreeing with our AFM and transmission electron microscopy (TEM) results (Figure 4 and Figure 5).

dx.doi.org/10.1021/ac2023537 |*Anal. Chem.* 2011, 83, 8787–8793

The fluorescence quenching of GO by DA also followed a typical Stern−Volmer type equation:

$$\frac{I_0}{I} = 1 + K_{sv}[DA] \quad (2)$$

where I and I_0 are the fluorescence intensity of GO in the presence and absence of DA, respectively, and K_{SV} is the Stern−Volmer quenching constant. The plot of I_0/I at 660 nm against [DA] shows a linear range from 0.25 to 20 μM with a K_{SV} value of 8.3 × 10^4 M^{-1} (Figure 3d). The fact that DA substantially quenched the near-IR fluorescence of GO with a blue-shift indicates a strong interaction between the excited-state GO and the attached DA molecules.

Self-Assembly of DA molecules on GO Nanosheets. The topographical changes of GO upon its interaction with DA were revealed by AFM and TEM images (Figure 4 and 5). In the absence of DA, the integrative GO flat nanosheets exhibited an average thickness of about 1.0 nm, indicating a fully exfoliated GO single layer.[44]

Addition of DA caused obvious corrugations of GO due to the self-assembly of DA molecules on the GO surface and a significant topographical change along with a height increment of approximately 0.3 nm comparable to the thickness of a single DA molecule, suggesting that dopamine molecules were adsorbed on the GO nanosheets as a monolayer or sub-monolayer.

The presence of vibrational features of the functional groups in both GO and DA in the FT-IR spectra further confirmed the formation of the DA−GO complex via multiple noncovalent interactions (Figure 6). GO gave a band at 1625 cm^{-1} for the stretching vibration of C═C in the unoxidized graphitic domain, 3426 cm^{-1} for the -OH vibration stretching, 1733 and 1391 cm^{-1} for carboxyl C═O and C−O, respectively, 1288 cm^{-1} for epoxy C−O, and 1076 cm^{-1} for alkoxy C−O groups at the edges of the GO sheets. DA gave characteristic bands at 3265 and 954 cm^{-1} corresponding to the -NH^{3+} vibration stretching and -CH_2, respectively, the bands at 1619 and 1500 cm^{-1} for the stretching vibration of C═C of the benzene ring of DA, and -OH vibration stretching of diols of DA, respectively. The GO−DA complex not only showed the bands of GO at 3426 (-OH), 1728 (carboxyl C═O), and 1619 cm^{-1} (C═C in the unoxidized graphitic domain) but also offered the bands of DA at 3265 and 2954 cm^{-1} for−NH_3^+ vibration stretching and -CH_2, respectively.

In addition, the GO−DA complex gave a band at 1515 cm^{-1}, 15 cm^{-1} frequency higher than that for -OH vibration stretching of diols in DA alone, likely due to the hydrogen-bonding interaction of the diols in DA with GO. The band for the stretching vibration of C═C in the unoxidized graphitic domain of the DA−GO complex gave a slightly lower frequency (1619 cm^{-1}) than that in free GO (1625 cm^{-1}) mainly because of the strong multiple noncovalent interactions between GO and DA.

Quenching Mechanism of DA on the Vis−Near-IR Fluorescence of GO. The fact that DA substantially quenched the near-IR fluorescence of GO with a blue shift indicates a strong interaction between the excited-state GO and the attached DA molecules. The fluorescence quenching of the excited-state GO may result from either PCT or FRET. We can exclude FRET as a possible mechanism for GO fluorescence quenching because of no overlap between the absorption spectra of DA and the emission spectra of GO (Figure 7a). The simultaneous change of the emission intensities of both GO and DA (Figure 7b) suggests that the fluorescence quenching was caused by electronic interaction upon DA attachment to GO.[46] This conclusion is also consistent with the fact that the fluorescence quenching of GO was not accompanied by a complementary growth of the fluorescence of DA (Figure 7b) and no absorbance of GO was lost (Figure S2 in the Supporting Information).[47] Instead, the fluorescence of both GO and DA was simultaneously quenched. GO also gave a significant quenching effect on the ultraviolet fluorescence of DA without the bleaching of the DA ground-state

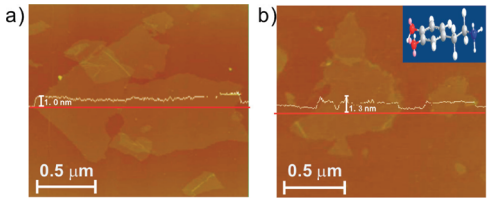

Figure 4. Tapping mode AFM images on mica: (a) free GO nanosheets; (b) GO−DA complex. Inset refers to a 3D view of DA molecule structure.

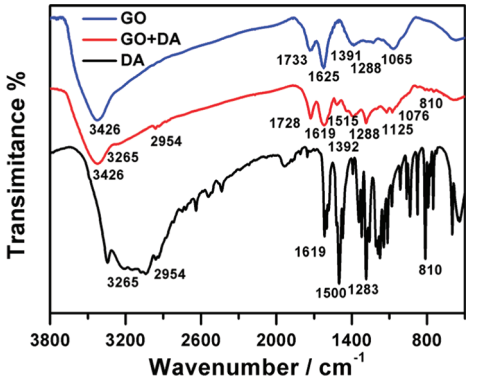

Figure 6. FT-IR spectra of GO (blue), DA (black), and the GO−DA complex (red).

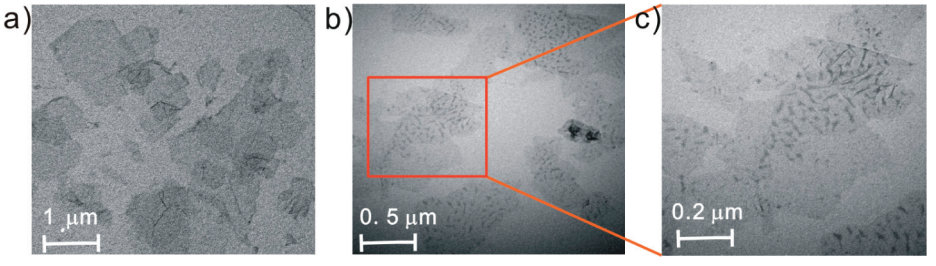

Figure 5. Representative TEM images of free GO nanosheets (a) and the GO−DA complex (b, c), showing obvious corrugations formed on the GO surface and suggesting self-assembly of DA molecules on the GO surface.

dx.doi.org/10.1021/ac2023537 |Anal. Chem. 2011, 83, 8787–8793

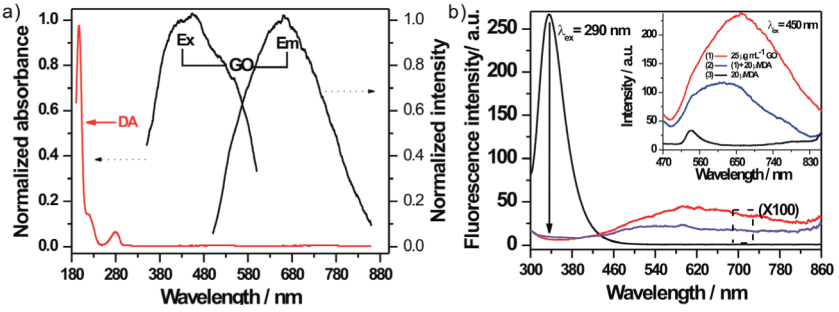

Figure 7. (a) UV−vis−near-IR absorption spectra of DA (red), fluorescence excitation and emission spectra of GO (black); (b) steady-state fluorescence spectra of 20 μM DA (black), 25 μg mL^{-1} GO (red), and the mixture of GO and DA (blue) in a pH 5.0 of 5.0 mM Tris-HCl solution under excitation of 290 nm in a high pass of 300 nm filter (inset: under excitation of 450 nm).

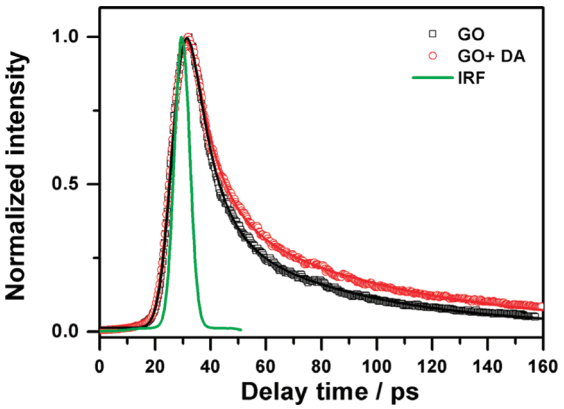

Figure 8. Time-resolved fluorescence decays of GO and the GO−DA complex in a scanning range of 160 ps with an instrument response function (IRF) of 4 ps. Excitation was accomplished using a frequency doubled Ti:sapphire laser pulse at 415 nm with a repetition rate of 76 MHz. Other conditions: buffer, 5.0 mM Tris-HCl solution at pH 5.0; DA concentration, 10 μM; λ_{ex}, 415 nm; λ_{em}, 660 nm.

absorption (Figure S3 in the Supporting Information), suggesting an efficient and rapid back-electron transfer from the attached DA to the GO,[44] which was further confirmed by time-resolved fluorescence spectroscopy.

Figure 8 shows only a peculiar ultrafast decay at the picosecond range for the near-IR emission of GO, distinct from the nanosecond decay of the blue photoluminescence of GO and other luminescent carbon nanomaterials,[48] suggesting that near-IR fluorescence of GO shared a different luminescence origin. Fitting the time-resolved fluorescence spectra with three decay components gave a major ultrafast component with a time constant of ~6 ps, 66% for free GO, and 74% for the GO−DA complex (Table 1). We ascribed the significant increase of the ultrafast process to the charge transfer from the excited GO to the attached DA molecules, resulting in near-IR fluorescence quenching of GO.[46,49] Additionally, increase of temperature led to a slight decrease of the quenching effect of DA on the fluorescence of GO (Figure S4 in the Supporting Information). These results suggest that the PCT quenching behavior between GO and DA was more likely to be a static quenching process due to the strong multiple noncovalent interactions between GO and DA.[50]

Analytical Performance of the Developed GO-Based Biosensor for Detection of DA. The PCT-based quenching effect of DA on the near-IR fluorescence of GO allows us to develop a sensitive label-free biosensor for the detection of DA with a

Table 1. Decay Parameters of 25 μg mL^{-1} GO Solution in the Absence and Presence of DA (10 μM) Obtained by Three-Exponential Fitting [a]

	τ_1 (ps)	A_1 (%)	τ_2 (ps)	A_2 (%)	τ_3 (ps)	A_3 (%)
GO	5.8	66.2	37.4	30.0	>160	3.8
GO + DA	6.4	73.5	37.6	24.6	>160	1.9

[a] $F(t) = A_1e^{-t/\tau_1} + A_2e^{-t/\tau_2} + A_3e^{-t/\tau_3}$.

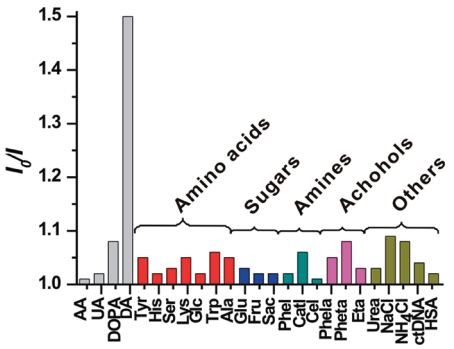

Figure 9. Response of the near-IR fluorescence of 25 μg mL^{-1} GO to the guest molecules at 5 μM in a pH 5.0 of 0.5 mM Tris-HCl solution, showing high selectivity to DA.

detection limit (3 s) of 94 nM (defined as the concentration of DA corresponding to the three times the standard deviation for 11 replicate detections of the blank solution) and a good precision (relative standard deviation) of 2.0% for 11 replicate detections of 2.0 μM DA. Moreover, the developed GO-based PCT fluorescence biosensor offers high selectivity for DA because of strong multiple noncovalent interactions between GO and DA (Figure 9). DA had significant quenching effect on the vis−near-IR fluorescence of GO. However, no significant change of the vis−near-IR fluorescence of GO whatsoever was detected in the presence of histidine (His), tyrosine (Tyr), tryptophan (Trp), alanine (Ala), lysine (Lys), glutamate (Glu), serine (Ser), glucose (Glc), fructose (Fru), saccharose (Sac), phenol (Phel), catechol (Catl), cyclohexanehexol (Cel), phenylamine (Phela), phenethylamine (Pheta), ethylamine (Eta), L-DOPA, AA, UA, urea, human serum albumin (HSA), and calf thymus DNA (ctDNA). Particularly, AA and UA, despite their similar electrochemical property to DA, did not affect the near-IR fluorescence of GO due to their low affinity to GO.[51,52] The

dx.doi.org/10.1021/ac2023537 |Anal. Chem. 2011, 83, 8787–8793

Table 2. Results for the Determination of Dopamine in Human Urine and Serum Samples

	DA concentration (μM)		
samples	spiked	measured (mean ± std dev, n = 3)	recovery (%) (mean ± std dev, n = 3)
human urine-1	0.0	nd[a]	
	5.0	5.1 ± 0.2	102.0 ± 4.0
	10.0	10.0 ± 0.3	100.0 ± 3.0
human urine-2	0.0	nd	
	2.0	2.3 ± 0.1	115.0 ± 5.0
	5.0	4.9 ± 0.3	98.0 ± 6.0
human serum-1	0.0	nd	
	2.0	2.2 ± 0.2	110.0 ± 10.0
	5.0	5.2 ± 0.2	104.0 ± 4.0
human serum-2	0.0	nd	-
	2.0	2.1 ± 0.3	105.0 ± 15.0
	5.0	5.1 ± 0.2	102.0 ± 4.0

[a] Not detected.

above results suggest that the developed GO-based PCT fluorescent biosensor enables highly favorable and specific fluorescence recognition of DA comparable to synthetic receptors.[53,54]

The developed GO-based PCT label-free near-IR fluorescent biosensor was employed for selective and sensitive detection of DA in biological fluids such as urine and serum samples. Negligible fluorescence background at 660 nm under excitation of 450 nm was observed in urine and serum samples (Figure S5 in the Supporting Information). An appropriate (100-fold) dilution of urine and serum was found sufficient to obtain a quantitative recovery (98−115%) of spiked DA and to use a simple aqueous standard solution for the accurate quantification of DA (Table 2).

CONCLUSIONS

In conclusion, we have explored the near-IR fluorescence of GO as a label-free PCT-based biosensor for DA. The multiple noncovalent interactions between GO and DA resulted in effective self-assembly of DA on the surface of GO, and significant fluorescence quenching, allowing development of a simple label-free PCT-based near-IR fluorescence biosensor for selective and sensitive detection of DA in biological fluids. This work may open a new possibility for development of PCT-based biosensors with direct readout of the near-IR fluorescence of GO.

ASSOCIATED CONTENT

Supporting Information. Additional information as noted in the text. This material is available free of charge via the Internet at http://pubs.acs.org.

AUTHOR INFORMATION

Corresponding Author
*Fax: (86)22-23506075. E-mail: xpyan@nankai.edu.cn.

ACKNOWLEDGMENT

This work was supported by the National Basic Research Program of China (Grant 2011CB707703), the National Natural Science Foundation of China (Grants 20935001 and 11074016), the Fundamental Research Funds for the Central Universities, and the Tianjin Natural Science Foundation (Grant 10JCZDJC16300).

REFERENCES

(1) Cai, W.; Piner, R. D.; Stadermann, F. J.; Park, S.; Shaibat, M. A.; Ishii, Y.; Yang, D.; Velamakanni, A.; An, S. J.; Stoller, M.; An, J.; Chen, D.; Ruoff, R. S. *Science* **2008**, *321*, 1815–1817.
(2) Gao, W.; Alemany, L. B.; Ci, L. J.; Ajayan, P. M. *Nat. Chem.* **2009**, *1*, 403–408.
(3) Casabianca, L. B.; Shaibat, M. A.; Cai, W. W.; Park, S.; Piner, R.; Ruoff, R. S.; Ishii, Y. *J. Am. Chem. Soc.* **2010**, *132*, 5672–5676.
(4) Dikin, D. A.; Stankovich, S.; Zimney, E. J.; Piner, R. D.; Dommett, G. H. B.; Evmenenko, G.; Nguyen, S. T.; Ruoff, R. S. *Nature* **2007**, *448*, 457–460.
(5) Paredes, J. I.; Villar-Rodil, S.; Martinez-Alonso, A.; Tascon, J. M. D. *Langmuir* **2008**, *24*, 10560–10564.
(6) Liu, Z.; Robinson, J. T.; Sun, X.; Dai, H. *J. Am. Chem. Soc.* **2008**, *130*, 10876–10877.
(7) Mohanty, N.; Berry, V. *Nano Lett.* **2008**, *8*, 4469–4476.
(8) Zhou, M.; Zhai, Y. M.; Dong, S. J. *Anal. Chem.* **2009**, *81*, 5603–5613.
(9) Xu, Y.; Liu, Z.; Zhang, X.; Wang, Y.; Tian, J.; Huang, Y.; Ma, Y.; Zhang, X.; Chen, Y. *Adv. Mater.* **2009**, *21*, 1275–1279.
(10) Swathi, R. S.; Sebastian, K. L. *J. Chem. Phys.* **2008**, *129*, No. 054703.
(11) Swathi, R. S.; Sebastian, K. L. *J. Chem. Phys.* **2009**, *130*, No. 086101.
(12) Lu, C. H.; Yang, H. H.; Zhu, C. L.; Chen, X.; Chen, G. N. *Angew. Chem., Int. Ed.* **2009**, *48*, 4785–4787.
(13) He, S.; Song, B.; Li, D.; Zhu, C.; Qi, W.; Wen, Y.; Wang, L.; Song, S.; Fang, H.; Fan, C. *Adv. Funct. Mater.* **2010**, *20*, 453–459.
(14) Lu, C. H.; Li, J.; Liu, J. J.; Yang, H. H.; Chen, X.; Chen, G. N. *Chem.—Eur. J.* **2010**, *16*, 4889–4894.
(15) Dong, H.; Gao, W.; Yan, F.; Ji, H.; Ju, H. *Anal. Chem.* **2010**, *82*, 5511–5517.
(16) Li, F.; Huang, Y.; Yang, Q.; Zhong, Z.; Li, D.; Wang, L.; Song, S.; Fan, C. *Nanoscale* **2010**, *2*, 1021–1026.
(17) Chang, H.; Tang, L.; Wang, Y.; Jiang, J.; Li, J. *Anal. Chem.* **2010**, *82*, 2341–2346.
(18) Wang, Y.; Li, Z.; Hu, D.; Lin, C.-T.; Li, J.; Lin, Y. *J. Am. Chem. Soc.* **2010**, *132*, 9274–9276.
(19) Jang, H.; Kim, Y.-K.; Kwon, H.-M.; Yeo, W.-S.; Kim, D.-E.; Min, D.-H. *Angew. Chem., Int. Ed.* **2010**, *49*, 5703–5707.
(20) Zhang, C.; Yuan, Y.; Zhang, S.; Wang, Y.; Liu, Z. *Angew. Chem., Int. Ed.* **2011**, *50*, 6851–6854.
(21) Song, Y.; Qu, K.; Zhao, C.; Ren, J.; Qu, X. *Adv. Mater.* **2010**, *22*, 2206–2210.
(22) Wen, Y. Q.; Xing, F. F.; He, S. J.; Song, S. P.; Wang, L. H.; Long, Y. T.; Li, D.; Fan, C. H. *Chem. Commun. (Cambridge, U. K.)* **2010**, *46*, 2596–2598.
(23) Fan, F.-R. F.; Park, S.; Zhu, Y.; Ruoff, R. S.; Bard, A. *J. Am. Chem. Soc.* **2008**, *131*, 937–939.
(24) Lui, C. H.; Mak, K. F.; Shan, J.; Heinz, T. F. *Phys. Rev. Lett.* **2010**, *105*, 127404–127407.
(25) Stöhr, R. J.; Kolesov, R.; Pflaum, J.; Wrachtrup, J. *Phys. Rev. B* **2010**, *82*, 121408–121411 (R).
(26) Liu, W.-T.; Wu, S. W.; Schuck, P. J.; Salmeron, M.; Shen, Y. R.; Wang, F. *Phys. Rev. B* **2010**, *82*, 081408–081411 (R).
(27) Sun, X.; Liu, Z.; Welsher, K.; Robinson, J.; Goodwin, A.; Zaric, S.; Dai, H. *Nano Res.* **2008**, *1*, 203–212.
(28) Luo, Z. T.; Vora, P. M.; Mele, E. J.; Johnson, A. T. C.; Kikkawa, J. M. *Appl. Phys. Lett.* **2009**, *94*, 111909-1–111909-3.
(29) Eda, G.; Lin, Y. Y.; Mattevi, C.; Yamaguchi, H.; Chen, H. A.; Chen, I. S.; Chen, C. W.; Chhowalla, M. *Adv. Mater.* **2010**, *22*, 505–509.

(30) Loh, K. P.; Bao, Q.; Eda, G.; Chhowalla, M. *Nat. Chem.* **2010**, *2*, 1015–1024.
(31) Liu, F.; Choi, J. Y.; Seo, T. S. *Biosens. Bioelectron.* **2010**, *25*, 2361–2365.
(32) Jung, J.; Cheon, D.; Liu, F.; Lee, K.; Seo, T. *Angew. Chem., Int. Ed.* **2010**, *49*, 5708–5711.
(33) Thomas, J.; Sherman, D. B.; Amiss, T. J.; Andaluz, S. A.; Pitner, J. B. *Bioconjugate Chem.* **2007**, *18*, 1841–1846.
(34) Ligett, S. B. *Pharmacology* **2000**, *61*, 167–173.
(35) Bock, M. G.; Patane, M. A. *Annu. Rep. Med. Chem.* **2000**, *35*, 221–230.
(36) Gingrich, J. A.; Caron, M. G. *Annu. Rev. Neurosci.* **1993**, *16*, 299–321.
(37) Shao, Y.; Wang, J.; Wu, H.; Liu, J.; Aksay, I. A.; Lin, Y. *Electroanalysis* **2010**, *22*, 1027–1036.
(38) Shang, N. G.; Papakonstantinou, P.; McMullan, M.; Chu, M.; Stamboulis, A.; Potenza, A.; Dhesi, S. S.; Marchetto, H. *Adv. Funct. Mater.* **2008**, *18*, 3506–3514.
(39) Hummers, W. S.; Offeman, R. E. *J. Am. Chem. Soc.* **1958**, *80*, 1339.
(40) Cote, L. J.; Kim, F.; Huang, J. X. *J. Am. Chem. Soc.* **2009**, *131*, 1043–1049.
(41) Clark, B. J.; Frost, T. Russell, M. A. *UV Spectroscopy: Techniques, Instrumentation, Data Handling/UV Spectrometry Group*; Chapman & Hall: London, New York, 1993; Vol. 4.
(42) Radu, D. R.; Lai, C.-Y.; Wiench, J. W.; Pruski, M.; Lin, V. S. Y. *J. Am. Chem. Soc.* **2004**, *126*, 1640–1641.
(43) Chen, J.-L.; Yan, X.-P. *Chem. Commun. (Cambridge, U. K.)* **2011**, *47*, 3135–3137.
(44) Stankovich, S.; Dikin, D. A.; Piner, R. D.; Kohlhaas, K. A.; Kleinhammes, A.; Jia, Y.; Wu, Y.; Nguyen, S. T.; Ruoff, R. S. *Carbon* **2007**, *45*, 1558–1565.
(45) Ohno, Y.; Maehashi, K.; Yamashiro, Y.; Matsumoto, K. *Nano Lett.* **2009**, *9*, 3318–3322.
(46) Sykora, M.; Petruska, M. A.; Alstrum-Acevedo, J.; Bezel, I.; Meyer, T. J.; Klimov, V. I. *J. Am. Chem. Soc.* **2006**, *128*, 9984–9985.
(47) Satishkumar, B. C.; Brown, L. O.; Gao, Y.; Wang, C. C.; Wang, H. L.; Doorn, S. K. *Nat. Nanotechnol.* **2007**, *2*, 560–564.
(48) Pan, D. Y.; Zhang, J. C.; Li, Z.; Wu, M. H. *Adv. Mater.* **2010**, *22*, 734–738.
(49) Cao, A.; Liu, Z.; Chu, S.; Wu, M.; Ye, Z.; Cai, Z.; Chang, Y.; Wang, S.; Gong, Q.; Liu, Y. *Adv. Mater.* **2010**, *22*, 103–106.
(50) Lakowicz, J. R. *Principles of Fluorescence Spectroscopy*, 3rd ed.; Springer: New York, 2006; pp 277−287.
(51) Wang, Y.; Li, Y.; Tang, L.; Lu, J.; Li, J. *Electrochem. Commun.* **2009**, *11*, 889–892.
(52) Hou, S.; Kasner, M. L.; Su, S.; Patel, K.; Cuellari, R. *J. Phys. Chem. C* **2010**, *114*, 14915–14921.
(53) Herm, M.; Molt, O.; Schrader, T. *Angew. Chem., Int. Ed.* **2001**, *40*, 3148–3151.
(54) Kolusheva, S.; Molt, O.; Herm, M.; Schrader, T.; Jelinek, R. *J. Am. Chem. Soc.* **2005**, *127*, 10000–10001.